Earth's Future

RESEARCH ARTICLE
10.1029/2022EF003219

Key Points:
- Major parts of the city of Lagos are subsiding at rates of more than 4 mm/yr
- Our analysis suggests a causal relationship between incidences of building collapse and differential subsidence in Lagos
- By 2053, a total area of 45 km^2 and approximately 2,200 buildings will be exposed to a high to very high risk of collapse

Supporting Information:
Supporting Information may be found in the online version of this article.

Correspondence to:
L. O. Ohenhen,
ohleonard@vt.edu

Citation:
Ohenhen, L. O., & Shirzaei, M. (2022). Land subsidence hazard and building collapse risk in the coastal city of Lagos, West Africa. *Earth's Future*, *10*, e2022EF003219. https://doi.org/10.1029/2022EF003219

Received 19 SEP 2022
Accepted 28 OCT 2022

Author Contributions:
Conceptualization: L. O. Ohenhen, M. Shirzaei
Formal analysis: L. O. Ohenhen, M. Shirzaei
Funding acquisition: M. Shirzaei
Investigation: L. O. Ohenhen, M. Shirzaei
Methodology: L. O. Ohenhen, M. Shirzaei
Software: M. Shirzaei
Supervision: M. Shirzaei
Validation: M. Shirzaei
Visualization: L. O. Ohenhen, M. Shirzaei
Writing – original draft: L. O. Ohenhen, M. Shirzaei

Land Subsidence Hazard and Building Collapse Risk in the Coastal City of Lagos, West Africa

L. O. Ohenhen[1] and M. Shirzaei[1]

[1]Department of Geosciences, Virginia Tech, Blacksburg, VA, USA

Abstract Every year incidents of building collapse claim many lives and cause enormous financial losses around the world, which are often blamed on low-quality materials, non-compliance with standards, lack of oversight, and failure to enforce building codes. Here, we highlight the role of land subsidence in triggering unprecedented collapses in the city of Lagos, Nigeria, which has reported over 200 casualties during 152 building failures since 2005. We used acquisitions from radar satellites for 2018–2021 and provided data that link subsidence to foundation damage and high building failure risk in the region. We estimate that an area of 5–81 km^2 and 255–4,000 buildings are exposed to a high to very high risk of collapse for short-term (10 years) to long-term (75 years) periods. Differential land subsidence can trigger building collapse, and the data presented here will enable authorities to create adequate building codes and standards and devise mitigation strategies.

Plain Language Summary Low-quality materials, non-compliance with standards, a lack of oversight, and failure to enforce construction codes are frequently cited as causes of the annual global increase in building collapses that kill countless lives and result in tremendous financial losses. In this article, we focus on the impact that land subsidence plays in causing building collapses in Lagos, Nigeria. We employed radar satellite acquisitions from 2018 to 2021 to present evidence linking subsidence with foundation damage and a significant risk of building failure in the area. We calculate that in the future, between 5 and 81 km^2 and 255–4,000 buildings are at a high to very high risk of collapsing.

1. Introduction

Building collapse is a common phenomenon often resulting from the structural failure of a building, culminating in its collapse. Worldwide, multiple events of building collapse are recorded each year, with an average of eight building collapses per year, resulting in greater than 300 deaths each year (Keim, 2021). Lagos, Nigeria, the third most populous coastal city in the world and the second most populated city in Africa (Figures 1a and 1b), with an estimated population of ∼15 million, has recorded an unabating incidence of building collapse over the past 50 years. The existing literature reports approximately 300 collapsed buildings between 1978 and 2022 in Lagos (Ebehikhalu & Dawam, 2014; Okunola, 2021), with more than 400 deaths, 6,000 displaced households, and an estimated loss of property worth about US$ 3.2 trillion (Okunola, 2021, 2022). Four such major incidences of collapsed buildings in Lagos have resulted in the loss of 191 lives (Figure 1c). Despite the significant socioeconomic and human impacts of these occurrences, incidences of building collapse in Nigeria are hugely underreported and do not receive major scholarly and media attention (Windapo & Rotimi, 2012). For example, a global report on building collapse over the last 50 years, reported only 12 collapsed buildings in Nigeria (Keim, 2021), which is 20 times less than the factual number of collapsed buildings (Akinyemi et al., 2016; Awoyera et al., 2021; Ebehikhalu & Dawam, 2014; Okunola, 2021; Oloke et al., 2017; Windapo & Rotimi, 2012).

In Nigeria, these occurrences have been a source of concern to stakeholders, leading to increased diffusion of engineering knowledge to examine the causes of building failure (Ebehikhalu & Dawam, 2014). The cause has majorly been attributed to carelessness, poor workmanship, design flaws, and the use of substandard construction materials (Adetunji et al., 2018; Ebehikhalu & Dawam, 2014; Okunola, 2021). However, a statistical comparison of three major cities with the highest rate of building collapse in Nigeria shows that incidences of building collapse in Lagos are 700%–1,900% (8–20 times) greater than in the other two cities (Akinyemi et al., 2016; Ede, 2010). This suggests an intrinsic process exclusive to the coastal city of Lagos that may be driving the incessant occurrence of building collapse.

Writing – review & editing: L. O. Ohenhen, M. Shirzaei

Subsidence, the lowering of land elevation, affects most megacities worldwide, with significant socioeconomic implications (Nicholls et al., 2021). More than 150 cities worldwide are experiencing subsidence of varying magnitude (rates up to tens of cm per year in some cities) (Wu et al., 2022; Zhou et al., 2020) and 15 of the 20 major coastal cities are at high risk of inundation due to subsidence (Herrera-García et al., 2021). Recently, the co-occurrence of subsidence and sea-level rise (SLR) in coastal cities has garnered greater attention due to the potential for increased future inundation hazards resulting from relative SLR (Miller & Shirzaei, 2021; Nicholls et al., 2021; Restrepo-Ángel et al., 2021; Shirzaei & Bürgmann, 2018; Shirzaei et al., 2021; Wu et al., 2022). However, subsidence is a more immediate problem in many regions than climate-induced SLR, particularly in areas experiencing rapid urbanization (Cian et al., 2019; Nicholls et al., 2021). Continuous subsidence may severely damage infrastructure (Fernández-Torres et al., 2020). The risk to infrastructure from subsidence is primarily due to spatially uneven settlements over the extent of the structure, for example, a building (Cigna & Tapete, 2021a; Ozer & Geurts, 2021). This inhomogeneous spatial subsidence causes an angular distortion, which may lead to the tilting, cracking, deformation, and failure of a building (Bjerrum, 1963; Burland et al., 1975; Ozer & Geurts, 2021). As a result, urban areas exposed to subsidence with high property densities are often expanding into vulnerable areas and structures are at risk of failure (Mohamadi et al., 2020).

Subsidence in Lagos has been documented by other authors and examined within the context of relative SLR-induced hazards, such as saltwater intrusion and the increased frequency of flooding (Cian et al., 2019; Ikuemonisan & Ozebo, 2020). In this contribution, we investigate the risk to buildings associated with subsidence in the coastal city of Lagos. We use measurements of vertical land motion (VLM) obtained from Interferometric Synthetic Aperture Radar (InSAR) collected between 2018 and 2021 to calculate the hazard associated with differential subsidence. This hazard map from subsidence is then combined with a building density map to create a structural-vulnerability risk map for Lagos and identify areas with a high risk of building collapse.

2. Materials and Methods

2.1. Building Collapse Data Set

We compiled a data set of building collapse locations for Lagos. Our study uses a data set of 106 collapsed buildings in Lagos (Data Set S1 in Supporting Information S1), compiled from eight different studies (Adetunji et al., 2018; Akinyemi et al., 2016; Awoyera et al., 2021; Ayeni & Adedeji, 2015; Ebehikhalu & Dawam, 2014; Odeyemi et al., 2019; Oloke et al., 2017; Windapo & Rotimi, 2012) and three online news media including *Cable News Network*, *Vanguard Nigeria*, and *The Guardian*. The meta-analysis includes data on all collapsed buildings from 1978 to 2022. We screened the data to extract 43 collapsed buildings between 2000 and 2022 where the precise geographic coordinates could be extracted and the buildings were not under construction at the time of the collapse (Figure 1b).

2.2. SAR Analysis

We measured ground deformation in Lagos using multitemporal SAR interferometric analysis of the Sentinel-1 A/B C-band satellite. The SAR data set includes 109 and 106 images acquired in ascending (18 March 2018–28 October 2021) and descending (13 March 2018–23 October 2021) orbit geometry, respectively (Figure 1a). Using these data sets, we generated 603 interferograms for the ascending mode (average incidence angle = 39.29° and heading angle = 347.95° within the study area) and 530 interferograms for the descending mode (average incidence angle = 43.93° and heading angle = 192.05°). The maximum temporal and perpendicular baselines for the data sets are 400 days and 250 m, respectively.

We generated high-resolution time series of deformation for the ascending and descending data sets using a multitemporal wavelet-based InSAR algorithm (Shirzaei, 2013; Shirzaei & Bürgmann, 2012). To this end, the geometrical phase was calculated and removed using the 30-m Shuttle Radar Topography Mission digital elevation model (Farr et al., 2007) and the satellite's precise ephemeris data (Shirzaei & Bürgmann, 2012). Next, the time series of the complex interferometric phase noise was calculated in the wavelet domain and analyzed statistically to identify the elite pixels (Shirzaei, 2013). We then implemented an iterative 2D sparse phase unwrapping algorithm to obtain the absolute estimate of the phase change for the elite pixels. Each unwrapped interferogram was corrected for the effect of orbital error (Shirzaei & Walter, 2011) and the topography-correlated atmospheric delay (Shirzaei & Bürgmann, 2012). Using a robust regression, we inverted the phase changes from the interferograms

10.1029/2022EF003219

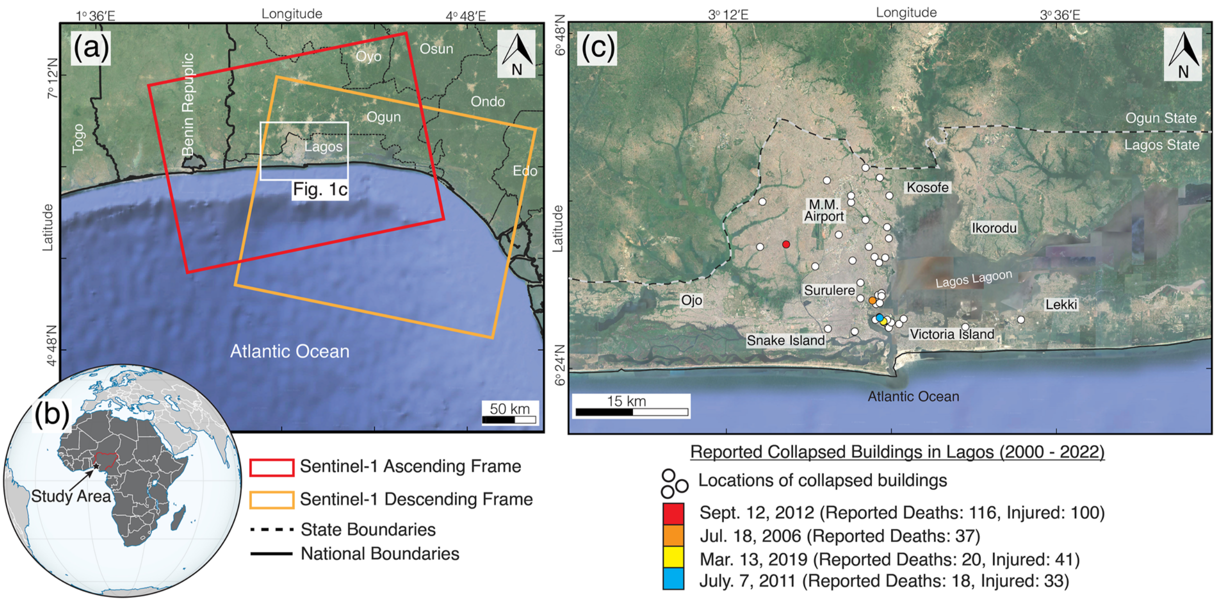

Figure 1. Study Area and Data sets. (a) Footprint of Synthetic Aperture Radar satellite images (Ascending and descending Sentinel-1A/B) in Lagos. (b) The location of Lagos in Nigeria and Africa. (c) Lagos map showing 43 geolocated collapsed buildings from 2000 to 2022 (white circles). The red, orange, yellow, and blue circles are locations of the 4 collapsed buildings with the highest reported casualty. The background image in panels (a and c) is satellite data from Google Earth.

and applied continuous wavelet transforms to reduce the temporal component of the atmospheric delay. Lastly, we calculated the velocities along the line-of-sight (LOS) direction for each elite pixel. The LOS displacement velocity is calculated as the slope of the best fitting line to the associated time series using a reweighted least squares estimation, with a reference point 21 km outside the city boundary (Figure S1 in Supporting Information S1). The final LOS displacement velocity and standard deviation for the ascending and descending data sets are shown in Figure S1 in Supporting Information S1.

The obtained LOS displacement velocity is composed of three components in the horizontal (east-west and north-south components) and vertical (uplift-subsidence component) directions. Given the near polar-orbiting satellites and a lack of up-to-date global navigation satellite system (GNSS) data, only the east-west and up-down components can be obtained reliably. Thus, we assume that motion in the north-south direction is negligible. Consequently, we combine ascending and descending LOS velocities to solve for east-west (E) and up-down (U) rates (Miller & Shirzaei, 2015).

To this end, we first identified co-located pixels of LOS displacement velocity from the ascending and descending tracks to obtain two co-located LOS displacement velocities. The model to combine the ascending and descending LOS displacement velocities to generate a high-resolution and accurate map of the E and U velocities is given by Equation 1:

$$\begin{pmatrix} \mathrm{ASC_{LOS}} \\ \mathrm{DES_{LOS}} \end{pmatrix} = \begin{pmatrix} C_E^{\mathrm{ASC}} & C_U^{\mathrm{ASC}} \\ C_E^{\mathrm{DES}} & C_U^{\mathrm{DES}} \end{pmatrix} \begin{pmatrix} E \\ U \end{pmatrix} \tag{1}$$

where, $\mathrm{ASC_{LOS}}$ and $\mathrm{DES_{LOS}}$ are the ascending and descending Sentinel-1 LOS displacement velocities, respectively. C are unit vectors projecting the displacement onto the LOS (Hanssen, 2001), which are functions of the incidence and heading angles. The final solution to Equation 1 is given by Equation 2:

$$X = A^{-1}L \tag{2}$$

Where,

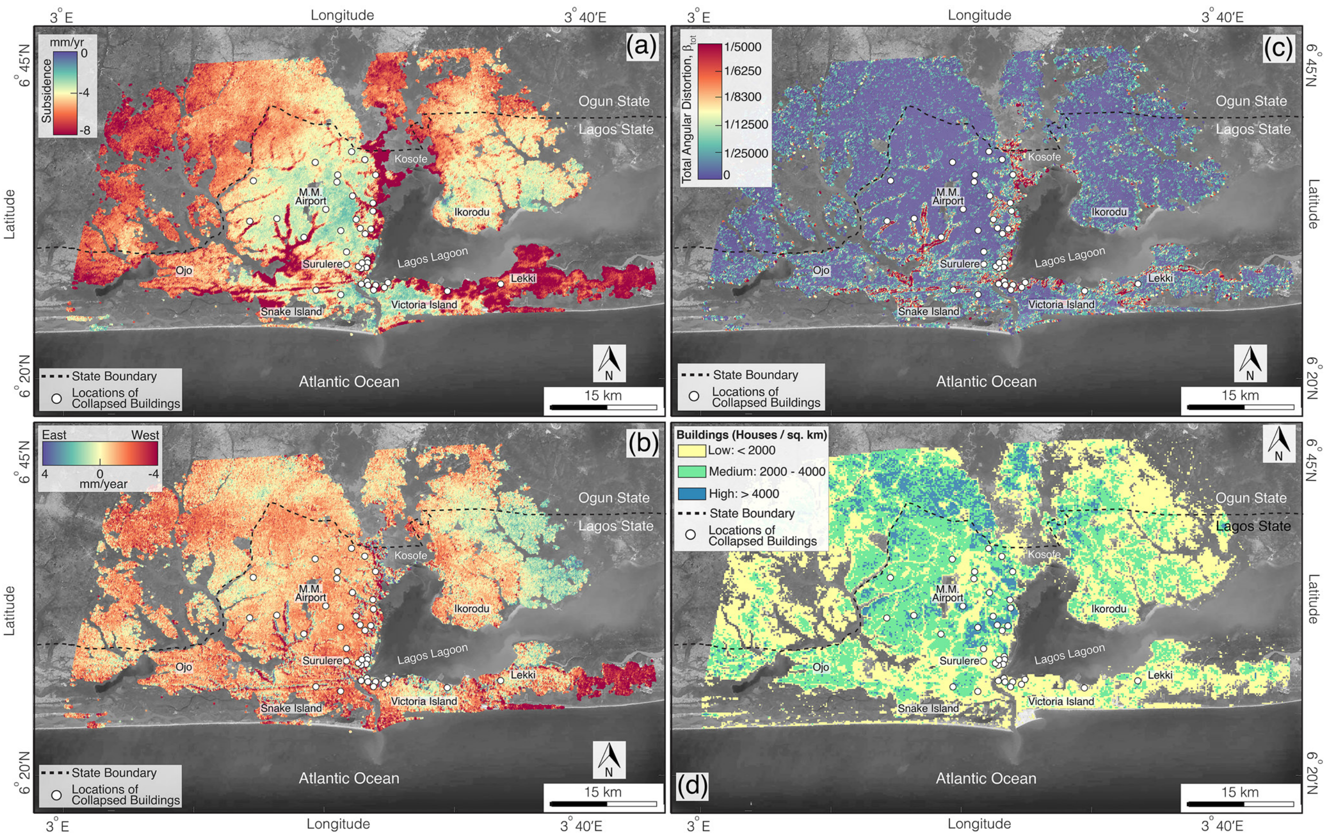

Figure 2. Spatial maps of 2D velocity, subsidence-induced hazard, and elements at risk in Lagos. (a) Vertical and (b) east displacement rates relative to the reference point (latitude: 6.87027° and longitude: 3.190534°). (c) Total angular distortion, β_{tot} for a 4 year period (2018–2021) and (d) building densities. The white circles are the locations of 43 collapsed buildings from 2000 to 2022. The background image in panels (a–d) is satellite data from Google Earth.

$$X = (EU)^T, A = \begin{pmatrix} C_E^{\mathrm{ASC}} & C_U^{\mathrm{ASC}} \\ C_E^{\mathrm{DES}} & C_U^{\mathrm{DES}} \end{pmatrix}, L = \begin{pmatrix} \mathrm{ASC_{LOS}} \\ \mathrm{DES_{LOS}} \end{pmatrix} \tag{3}$$

The resulting VLM rate and east velocity are shown in Figures 2a and 2b.

2.3. Assessing Structure Damage Risk Due To Differential Subsidence

To assess the risk level that buildings are exposed to due to land subsidence, we adopt the risk matrix. The risk matrix comprises 5 categories; R_0—Very low, R_1—Low, R_2—Medium, R_3—High, and R_4—Very high. In each category, a given hazard likelihood is related to hazard severity, namely building damage (Cigna & Tapete, 2021a). The severity of damage in Lagos is approximated using angular distortion (Burland et al., 1975; Skempton & Macdonald, 1956). The angular distortion is commonly applied in geotechnical engineering to estimate the severity of building damage associated with subsidence/differential settlement (e.g., Cigna & Tapete, 2021a; Fernández-Torres et al., 2020; Ozer & Geurts, 2021; Vassileva et al., 2021). Differential subsidence is a hazard to buildings, with the potential to cause significant damage, failure, and ultimately the collapse of buildings (Burland et al., 1975; Cigna & Tapete, 2021a; Fernández-Torres et al., 2020; Vassileva et al., 2021). Damage to buildings due to differential settlement is a result of strain changes between two adjacent points which causes angular distortion, a hazard to buildings (Burland et al., 1975; Vassileva et al., 2021).

Given l is the horizontal distance between adjacent InSAR pixels (75 m in this study) and δ is the differential vertical displacement between adjacent InSAR pixels, the angular distortion, β is given by Equation 4:

$$\beta = \frac{\delta}{l} \tag{4}$$

The calculated β at the location of each pixel is shown in Figure S2 in Supporting Information S1. Several β based on empirical data have been suggested as the critical value, which defines the threshold of negligible to very severe damage to buildings and infrastructure. Wood (1958) reported β of 1/1,000–1/100 as likely to cause cracks and damage to brick walls and encased steel frames. For brick-bearing walls, β greater than 3.25/1,000 will cause moderate to very severe damage (Boscardin & Cording, 1989). Structural damage appears in beams and columns when β exceeds 6.6/1,000 (Skempton & Macdonald, 1956), and β greater than 3.3/1,000 may cause cracking of walls in buildings with steel or reinforced concrete frames (Bjerrum, 1963; Day, 1990; Skempton & Macdonald, 1956).

It should be noted that β calculated using Equation 4 is the distortion rate affecting the buildings. To obtain the total distortion, β_{tot}, over the InSAR period (Figure 2c), we multiply the calculated angular distortion (Figure S2 in Supporting Information S1) with the period of 4 years. The β obtained for the InSAR period is only the partial distortion and does not reflect the total distortion accumulated over the lifetime of buildings (Cigna & Tapete, 2021a). To investigate future risks to building due to land subsidence, we examine different scenarios hypothesizing that the measured subsidence rate is continuous in the region. This hypothesis follows the assumption of a linear rate of VLM during the 21st century (Shirzaei et al., 2021), a widely used scenario for assessing future hazards, for instance, due to relative SLR (Fox-Kemper et al., 2021). To this end, given the values shown in Figure S2 in Supporting Information S1, we calculate the accumulated β_{tot} in Lagos over 10 years (hereafter short-term period: 2018–2028), 35 years (hereafter intermediate-term period: 2018–2053), and 75 years (hereafter long-term period: 2018–2093).

Next, we resample the β_{tot} on a 0.2 × 0.2 km grid, and following Cigna and Tapete (2021a), defined four classes: low ($0 \leq \beta_{tot} < 1/3{,}000$), medium ($1/3{,}000 \leq \beta_{tot} < 1/1{,}500$), high ($1/1{,}500 \leq \beta_{tot} \leq 1/500$), and very high ($\beta_{tot} > 1/500$), indicative of the increasing likelihood of damage (Figure S3 in Supporting Information S1). High β_{tot} identifies hot zones with the greatest strain changes. Typically, β_{tot} in excess of 1/3,000 is likely to cause structural damage (e.g., tilting and cracking) and foundational problems to buildings (Skempton & Macdonald, 1956; Zhang & Ng, 2007), and a critical β of 1/3,300 defines the damage threshold for sand-built structures (Burland et al., 1975).

To quantify the likelihood, we extracted the building footprint for Lagos from the Open Data Commons Open Database License (ODbL) available from Microsoft. Using the building density classification for urban housing in developing countries (Sanya & Mwebaze, 2020), we resample the building counts on the 0.2 × 0.2 km grid. We categorized building density into three classes with an increasing number of buildings per km^2: low ($0 \leq$ *building density* $< 2{,}000$), medium ($2{,}000 \leq$ *building density* $\leq 4{,}000$), and high (*building density* $> 4{,}000$) (Figure 2d). Using the β_{tot} and the building density, we then create the risk classifications for Lagos.

3. Results

3.1. Spatial Pattern of Subsidence

The spatial distribution of the VLM rate indicates broad-scale subsidence in Lagos (Figure 2a), with rates exceeding 4 mm/yr in most regions (Figure 3a), consistent with previous studies (Cian et al., 2019; Ikuemonisan & Ozebo, 2020; Mahmud et al., 2016). Subsidence hotspots with rates exceeding 6 mm/yr are noted along the coastline of the Atlantic Ocean, the southwestern region of Lagos; Lekki, the flood plains, and regions bounding the Lagos Lagoon (Figure 2a). To validate the observed InSAR measurement, we compared the VLM rate for an inactive GNSS station with data coverage between 2011 and 2013 with InSAR measurements between 2018 and 2021 (Figure S4 in Supporting Information S1). The VLM rate for the GNSS station (ULAG station) is the vertical rate obtained directly from the Nevada Geodetic Laboratory (Blewitt et al., 2016, 2018), while the InSAR VLM rate is obtained by averaging pixels within 100 m radius of the ULAG GNSS station (Figure S4 in Supporting Information S1). The comparison of the VLM rates shows a difference of 0.07 mm/yr (Figure S4 in Supporting Information S1).

The associated horizontal velocity, which measures motion in the east-west direction (Figure 2b) relative to the reference point (Figure S1 in Supporting Information S1) shows velocities of ±1 mm/yr for ~50% of the pixels (Figure 3b). However, enhanced east and west velocities are observed to cohere with some regions with high subsidence rates, such as the regions (Figures 2a and 2b). We further evaluate the subsidence rate at the location of 43 collapsed buildings between 2000 and 2022 where the precise geographic coordinates could be extracted,

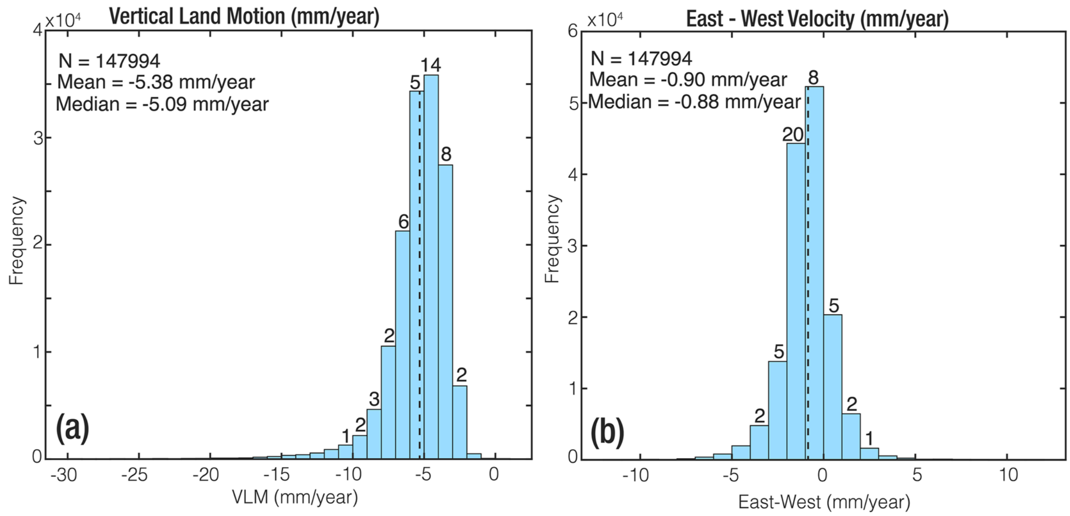

Figure 3. Distribution of 2D Velocity. (a) Histogram showing the distribution of vertical land motion rate (mm/yr). (b) Histogram showing the distribution of east-west velocity (mm/yr). The vertical lines on the histograms show the median velocity. The numbers on each bar are the number of collapsed buildings with the corresponding velocities.

and the buildings were not under construction at the time of the collapse (Figure 1c). The majority (>30) of the 43 geographically mapped collapsed buildings are located in areas with high subsidence rates and enhanced east-west velocities (Figures 2a, 2b, and 3). Additionally, the time series of VLM indicate continuous subsidence in all 43 locations of collapsed buildings, exceeding 30 mm in some locations (Figure S5 in Supporting Information S1). This observation may suggest a causal relationship between land subsidence and building collapse. However, we note that we cannot investigate this relationship further due to the lack of historical observation.

Noteworthy, the time series data (Figure S5 in Supporting Information S1) shows a change in the trend recorded toward the end of 2020, which may indicate a poroelastic response to change in groundwater use due to the increased/decreased groundwater use in 2020 during the Covid-19 lockdown or "Covid-effect."

3.2. Angular Distortion Assessment

Figure 2c shows the spatial distribution of the total accumulated angular distortion (β_{tot}) in Lagos for 4 years (2018–2021). The accumulated β_{tot} is low ($0 \leq \beta_{tot} < 1/3,000$), with only 0.7 km^2 of the city classified as a medium ($1/3,000 \leq \beta_{tot} \leq 1/1,500$) hazard zone (Figure S3a in Supporting Information S1). However, higher β_{tot} values (>1/5,000) are localized in some areas with subsidence rates exceeding 5 mm/yr, which indicates uneven subsidence rates in these regions (Figure 2c). While the β_{tot} for the 4 years period in Lagos is below the threshold of critical β of 1/3,300 for sand-built structures (Burland et al., 1975), the β_{tot} accumulates rapidly for short, intermediate, and long-term periods (Figures S3b–S3d in Supporting Information S1). For a short-term period (10 years: 2018–2028), the total area classified with low, medium, and high β_{tot} are 993.4, 67.8, and 8.2 km^2, respectively, with no area having very high β_{tot} values (Figure S3b in Supporting Information S1). The total area classified with low, medium, high, and very high β_{tot} for the intermediate term period (35 years: 2018–2053) are 753.6, 214.5, 93.5, and 8.0 km^2, respectively (Figure S3c in Supporting Information S1). For the long-term period (75 years: 2018–2093), the total area with low, medium, high, and very high β_{tot} are 606.6, 285.8, 147.9, and 29.2 km^2, respectively (Figure S3d in Supporting Information S1).

3.3. Building Collapse Risk Assessment

The produced risk maps for Lagos (Figure 4 and Table 1) are based on the hazard severity for the different periods (β_{tot}) combined with the building density in an area (Figure 4e). The different risk maps are due to the β_{tot} in four-time periods (InSAR period, short term, intermediate term, and long term periods). Here, we assume the building density to be immutable, however, the building density in Lagos is expected to increase with the projected population increase, which may exacerbate the risk to the region. From the risk map, the total areas with

10.1029/2022EF003219

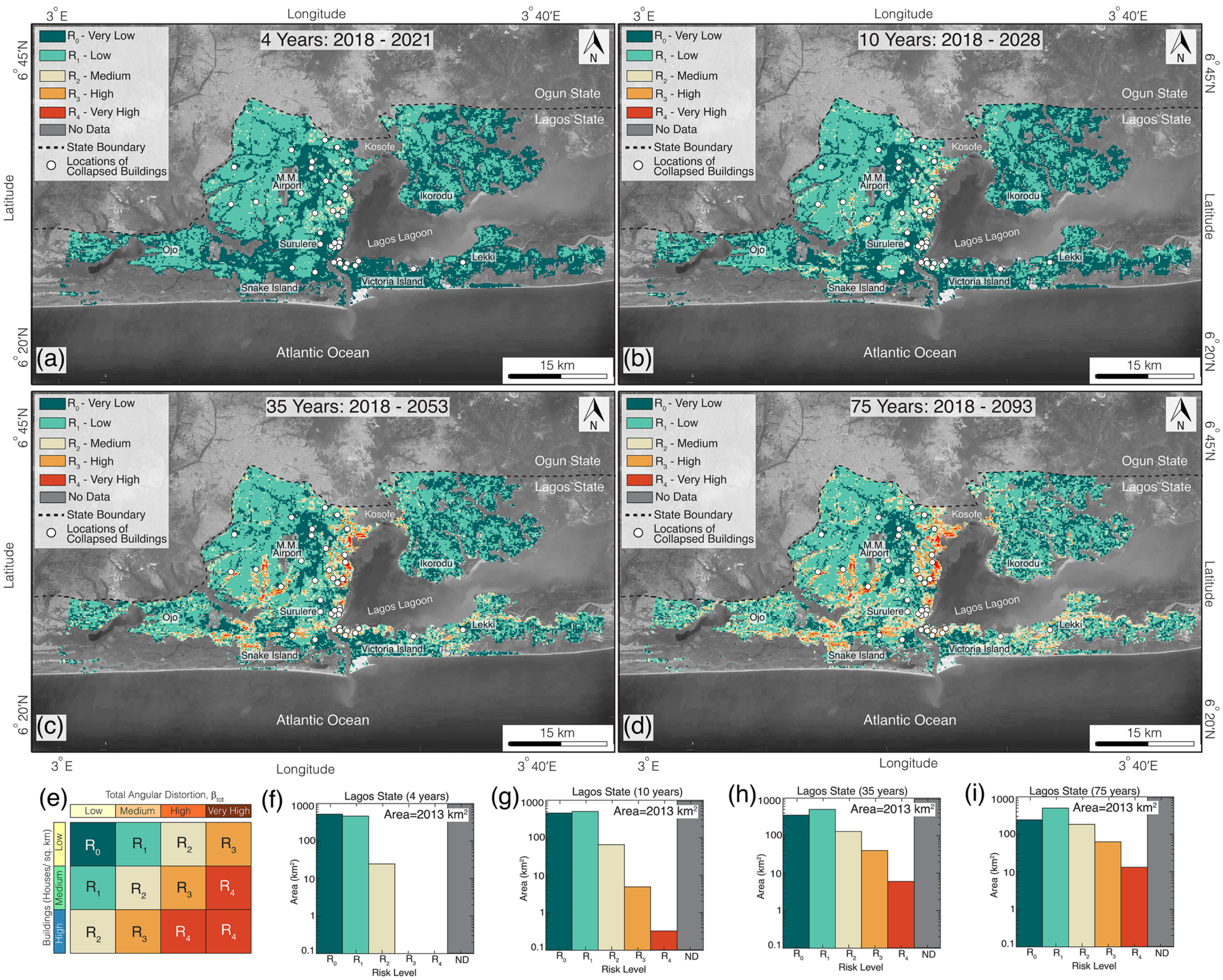

Figure 4. Risk maps for Lagos. Risk zoning of buildings at 0.2 km grid resolution for (a) Interferometric Synthetic Aperture Radar (InSAR) period (4 years: 2018–2021), (b) short-term (10 years: 2018–2028), (c) intermediate-term (35 years: 2018–2053), and (d) long-term (75 years: 2018–2093). (e) The risk matrix used to combine the total angular distortion (β_{tot}) and building density data to obtain the risk map. The exposure to the different risk level for (f) InSAR period (4 years: 2018–2021), (g) short-term (10 years: 2018–2028), (h) intermediate-term (35 years: 2018–2053), and (i) long-term (75 years: 2018–2093). The white circles are the locations of 43 collapsed buildings from 2000 to 2022. The risk level for 43 collapsed buildings are shown in Figure S6 in Supporting Information S1. The background image in panels (a–d) are satellite data from Google Earth.

very low-, low-, and medium-risk for a 4-year period are 540, 488, and 26 km^2, respectively, with no high-, and very high-risk areas (Figures 4a and 4f, Table 1). This risk increases over longer periods. Short-term, the high- and very high-risk areas are 5 and 0.3 km^2, respectively (Figures 4b and 4g, Table 1). The area of the high-risk zones for the intermediate and long-term periods are 39 and 67 km^2, respectively, with very high-risk areas of 6 and 14 km^2, respectively (Figures 4c, 4d, 4h, and 4i, Table 1). The spatial distribution of the 43 geographically mapped collapsed buildings shows that ∼50% or more of the collapsed buildings occur within the medium- to very high-risk zones for short-term to long-term scenarios (Figure S6 in Supporting Information S1).

Useful information for policymakers in assessing hazard zones is identifying high-risk-hazard-prone zones within each district (known as local government area; LGA in Nigeria). These statistical risk maps classified based on districts are essential resources for developing the most effective risk reduction and management strategies (Cigna & Tapete, 2021a) and urban development planning for the next 35 years. Here, we provide a useful risk map categorized by the 20 LGAs in Lagos utilizing the risk map for the intermediate-term period (Figure 5 and Table 2). The major LGAs with more than 1 km^2 of high- and very high-risk areas are Ajeromi, Alimosho,

Table 1
Area of Different Risk Levels in Lagos for Interferometric Synthetic Aperture Radar Period (4 Years: 2018–2021), Short Term (10 Years: 2018–2028), Intermediate-Term (35 Years: 2018–2053), and Long Term (75 Years: 2018–2093) Period

Risks	Four years	Ten years	Thirty-five years	Seventy-five years
Very low	539.6	496.6	347.3	259.1
Low	488.3	501.6	524.3	516.0
Medium	26.1	50.7	137.8	197.4
High	0.0	4.8	38.6	67.4
Very high	0.0	0.3	5.9	14.2
No data	958.9	958.9	958.9	958.9
Total (km^2)	2012.9	2012.9	2012.9	2012.9

Amuwo-Odofin, Eti-Osa, Ikorodu, Kosofe, Lagos Island, Lagos Island, Ojo, Oshodi, and Shomolu (Figure 5 and Table 2).

4. Discussion

The coastal city of Lagos is the largest in Nigeria, and the most populous coastal city in Africa, with a population of ∼15 million people. The incessant occurrence of building collapse in Lagos is an immediate and emerging threat to the population, infrastructure, and economy. Here, we provide the first structural risk map of Lagos using high-resolution measurements of VLM. There are certain limitations to our study, which help identify future research needs. First, the lack of a comprehensive data set for buildings in Lagos (such as the age of buildings and collapsed building database) provides uncertainties in our structural vulnerability analysis. Also inherent in our analysis is the assumption of a linearly continuous subsidence rate. VLM is dynamic and may decrease (or increase) even within short time scales (Figure S5 in Supporting Information S1), this change in the VLM may cause the

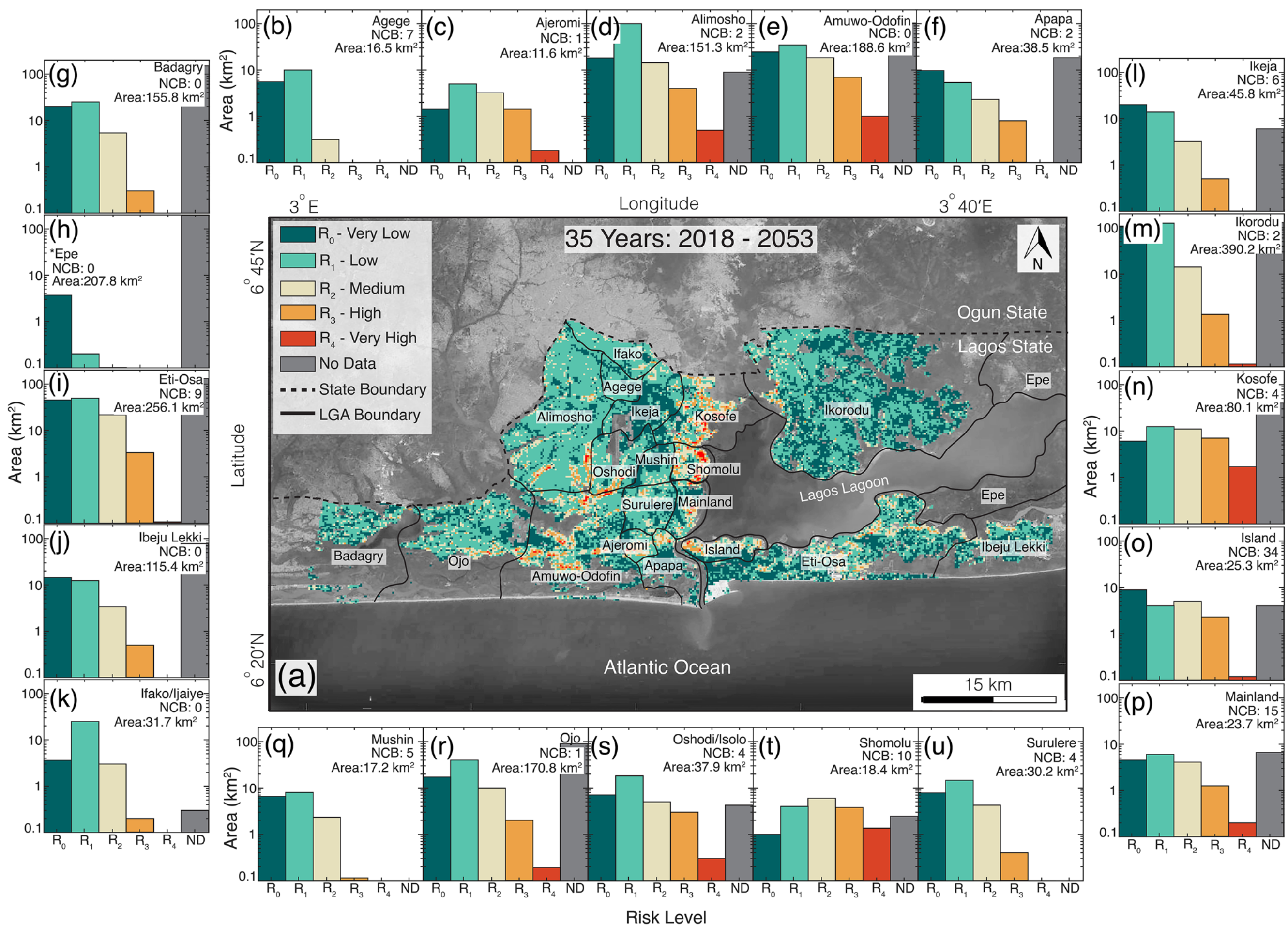

Figure 5. Thirty-five years (2018–2053) risk map categories for the 20 districts or local government areas (LGAs) in Lagos. (a) Risk map showing the boundaries for the different LGA. Risk levels for (b) Agege, (c) Ajeromi, (d) Alimosho, (e) Amuwo-Odofin, (f) Apapa, (g) Badagry, (h) Epe, (i) Eti-Osa, (j) Ibeju-Lekki, (k) Ifako/Ijaiye, (l) Ikeja, (m) Ikorodu, (n) Kosofe, (o) Lagos Island, (p) Lagos Mainland, (q) Mushin, (r) Ojo, (s) Oshodi/Isolo, (t) Shomolu, and (u) Surulere. *Epe LGA is undersampled with total spatial coverage less than 5 km^2. NCB is the number of collapsed buildings in each LGA (Data Set S1 in Supporting Information S1). The background image in panel (a) is satellite data from Google Earth.

Table 2
Area of 35 Years (2018–2053) Risk Map for Different Districts (or Local Government Areas) in Lagos

	Class						
LGAs	Very low	Low	Medium	High	Very high	No data	Total (km^2)
Agege	5.4	10.8	0.3	0.0	0.0	0.0	16.5
Ajeromi	1.6	5.2	3.0	1.5	0.2	0.0	11.6
Alimosho	19.5	103.2	14.5	4.1	0.5	9.5	151.3
Amuwo-Odofin	25.8	34.6	18.8	7.4	1.0	101.0	188.6
Apapa	10.1	5.6	2.4	0.8	0.0	19.5	38.5
Badagry	20.1	25.1	5.0	0.3	0.0	105.3	155.8
Epe	3.8	0.2	0.0	0.0	0.0	203.8	207.8
Eti-Osa	44.3	47	21.5	3.4	0.1	139.9	256.1
Ibeju Lekki	15.8	13.4	3.6	0.4	0.0	82.3	115.4
Ifako	3.4	24.4	3.4	0.2	0.0	0.3	31.7
Ikeja	20.3	16.2	3.1	0.5	0.0	5.7	45.8
Ikorodu	115.2	125.4	13.2	1.2	0.1	135.1	390.2
Kosofe	6.1	12.8	11.6	7.0	1.7	40.9	80.1
Lagos Island	8.6	4.4	5.5	2.2	0.1	4.4	25.3
Lagos Mainland	4.7	6.2	4.6	1.2	0.2	6.9	23.7
Mushin	6.6	8.3	2.2	0.1	0.0	0.0	17.2
Ojo	19.8	41.3	10.3	2.0	0.2	97.3	170.8
Oshodi/Isolo	7.3	18.7	4.6	2.6	0.3	4.5	37.9
Shomolu	1.0	4.0	6.1	3.4	1.4	2.6	18.4
Surulere	8.0	17.6	4.2	0.4	0.0	0.0	30.2
Total (km^2)	347.3	524.3	137.8	38.6	5.9	958.9	2012.9

Note. The risk levels for different districts for an InSAR period (4 years: 2018–2021), short term (10 years: 2018–2028), and long term (75 years: 2018–2093) period periods are shown in Tables S1–S3 in Supporting Information S1.

risk to buildings in Lagos to be lower or higher for different time intervals. Nevertheless, the current risk products for Lagos are valid under the current rates of VLM and building densities.

The spatial distribution of VLM shows broad-scale subsidence across Lagos. Two possible drivers of coastal subsidence in the region are natural compaction of Holocene sediments and compaction associated with the decrease in pore-fluid pressure due to fluid extraction (Blackwell et al., 2020; Khorrami et al., 2020; Minderhoud et al., 2020; Shirzaei et al., 2021). The geology along the Atlantic Ocean coasts and the bank of Lagos Lagoon comprise Holocene alluvium deposits (Ikuemonisan & Ozebo, 2020). The compaction of these unconsolidated sediments enhanced by the weight of the overburden may be driving subsidence in the region. This subsidence may be further accelerated by anthropogenic effects caused by the weight of the overlying city (Parsons, 2021) and fluid extraction associated with the unregulated exploitation of groundwater from the ∼150,000 boreholes in the region (Balogun et al., 2017; Ikuemonisan & Ozebo, 2020; Mahmud et al., 2016).

The observed subsidence in several locations in Lagos is a potential hazard to buildings, considering that total settlements greater than 51 mm may compromise the structural integrity of isolated building foundations on sand and clay soils (Skempton & Macdonald, 1956). Given the average subsidence rate of 5.4 mm/yr (Figure 3a), this threshold of total subsidence is exceeded for buildings older than 10 years. Differential subsidence can potentially cause the failure and collapse of buildings (Fernández-Torres et al., 2020; Vassileva et al., 2021). The accumulation of differential subsidence over a distance represented by β is a present hazard in Lagos and can potentially compromise the structural integrity of buildings. For example, several areas in Murtala Muhammad airport (M. M. Airport in Figures 1c and 2) are classified as high and very high hazard zones (Figures S3b–S3d in Supporting Information S1), which corresponds to the cracks observed in pillars within the airport (Figure S7a in Supporting Information S1). Additionally, studies based on visual inspection of buildings have identified cracked, sinking, and tilted foundations across Lagos city, located primarily in areas with subsidence rates exceeding 6 mm/yr and with the greatest differential subsidence for short-, intermediate-, and long-term periods, such as Kosofe (Figure 2a, Figures S7b–S7d in Supporting Information S1, Oloruntola et al., 2018; Oyedele et al., 2012).

The temporal evolution of the risk for short-term to long-term periods is indicative of current and future building collapse risk in Lagos. Considering a minimum building density in Lagos of 50 buildings/km^2, the minimum number of buildings at high- to very high-risk for short-term, intermediate-term, and long-term scenarios are 255, 2,250, and 4,050, respectively. This is significant in view of the large population in Lagos, almost double New York City's population. Over the last decade (2012–2022), the number of recorded casualties in Lagos from 44 collapsed buildings has exceeded 600 (337 deaths and 284 injuries), with 12 reported in 2022 (Data Set S1 in Supporting Information S1). There have been 100 documented building collapses in the last 35 years (1987–2022), resulting in 911 casualties (538 deaths and 373 injuries) (Data Set S1 in Supporting Information S1). This highlights the present and persistent threat to people residing in high-risk areas. We emphasize that a building residing in a high or very high-risk zone is not sufficient criteria to cause the collapse of a building. Other factors for consideration include the soil type and foundation materials (Skempton & Macdonald, 1956; Zhang & Ng, 2007), type of building construction material, the age, and maintenance state of the buildings (Cigna & Tapete, 2021a; Ozer & Geurts, 2021). Thus, the use of substandard building materials and poor maintenance culture of buildings prevalent in Lagos (Ayeni & Adedeji, 2015; Ede, 2010; Odeyemi et al., 2019; Okagbue et al., 2018; Okunola, 2021) are likely to unfavorably tilt the scales of a building from a low- to high-risk zone.

For a 35-year development plan, the high- and very high-risk zones within each LGA constitute hotspots for building collapse in Lagos. For example, in the Lagos Mainland and Island LGAs, while the high and very high-risk zones within these LGAs are less than 15% of the total area in the district, the total area of high- and very high-risk zones for Mainland and Island are 1.4 and 2.3 km^2, respectively capable of hosting more than 100 buildings. Three LGAs of particular concern, with a high risk, are Island (Figure 5o), Mainland (Figure 5p), and Shomolu (Figure 5t), with approximately 50% of the total area within the LGA having medium to very high risks and 10 or more reported incidence of collapsed buildings since 1978 (Data Set S1 in Supporting Information S1). Given the considerable number of reported collapsed structures (34 collapsed buildings), as well as the rapid expansion of population and infrastructure on Lagos Island, we categorize this area as an emergent high-risk zone disposed to the future incidence of collapse buildings and should be a focus of frequent monitoring. From a management and risk assessment standpoint, regular monitoring of VLM, building, and population changes are required to continuously update the derived risk map for the city.

Future studies exploiting the ages of buildings in Lagos will improve the derived products in this current study. Future investigations to map the soil mechanical properties of Lagos and detailed statistical analysis of building construction standards within Lagos would be useful to tease out the relative contribution of differential subsidence and substandard engineering practice to building collapse in Lagos.

Building failure occurs worldwide and poses a significant danger to lives and properties. In November 2012, a five-story building collapsed in Accra, Ghana, causing the death of 14 people, with 61 injuries (Boateng, 2020). The 2013 collapse of the eight-story Rana Plaza in Savar, Dhaka, Bangladesh, resulted in more than 1,100 deaths and an estimated 2,500 injuries (Kabir et al., 2019). In June 2021, the collapse of a twelve-story building in Miami, Florida, USA claimed the lives of 98 people (Lu et al., 2021). As cities expand, the effects of natural and anthropogenic subsidence are expected to increase, posing unprecedented risks to population and infrastructure. In response, monitoring surface deformation using remotely sensed techniques is essential to providing up-to-date subsidence hazard risk assessment maps (Blackwell et al., 2020; Cigna & Tapete, 2021a, 2021b; Fernández-Torres et al., 2020; Mohamadi et al., 2020; Vassileva et al., 2021; this study). Our analysis demonstrates the potential role of subsidence in causing the collapse of structures and in creating risk assessment maps for buildings in megacities experiencing subsidence. These maps are invaluable in informing policy decisions about priority risk reduction and adaptation strategies and identifying the most vulnerable communities.

5. Conclusion

In this study, measurements of vertical ground motion using radar satellite observation from 2018 to 2021 show a subsidence rate of more than 4 mm/yr in most parts of Lagos, West Africa. We synthesized the subsidence hazard and building density maps to create the first structural vulnerability map for the region and provide evidence suggesting differential land subsidence plays a role in frequent incidences of building collapse in Lagos. Our analysis shows that an area of 5–81 km^2 and 255–4,050 buildings are exposed to a high- to very high risk of collapse for a 10–75 years period. This poses a significant threat to the more than 15 million people in Lagos and highlights the vulnerability of sinking megacities worldwide.

Data Availability Statement

The ascending (Path 1, Frame 1200) and descending (Path 95, Frame 571) SAR data sets are obtained from the Alaska Satellite Facilities (https://search.asf.alaska.edu/#/). The tabular collapsed building, VLM data, and the risk maps necessary to evaluate the conclusions in the paper are available at https://doi.org/10.7294/19738957. The building footprint data used to create the building density map is available from Microsoft under the Open Data Commons Open Database License, and the vector tile is available from ArcGIS (https://www.arcgis.com/home/item.html?id=f40326b0dea54330ae39584012807126).

Acknowledgments

We would like to thank Florence *Nkem* Onyike for her help with compiling the collapsed building data set. We thank the two anonymous reviewers for their insightful comments and suggestions. L.O. and M.S. are supported by the National Aeronautics and Space Administration (NASA) Grant 80NSSC170567.

References

Adetunji, M. A., Oyeleye, O. I., & Akindele, O. A. (2018). Assessment of building collapse in Lagos Island, Nigeria. *American Journal of Sustainable Cities and Society*, *1*(7), 18–28. https://doi.org/10.26808/rs.aj.i7v1.04

Akinyemi, A. P., Dare, G. M., Anthony, A. I., & Dabara, D. I. (2016). Building collapse in Nigeria: Issues and challenges. In *Conference of the International Journal of Arts & Sciences*, (Vol. *9*, No. (1), pp. 99–108). Retrieved from http://ssrn.com/abstract=2784266

Awoyera, P. O., Alfa, J., Odetoyan, A., & Akinwumi, I. I. (2021). Building collapse in Nigeria during recent years: Causes, effects, and way forward. In *IOP Conference Series: Materials Science and Engineering*, (Vol. 1036, No. (1), p. 012021). IOP Publishing. https://doi.org/10.1088/1757-899x/1036/1/012021

Ayeni, D. A., & Adedeji, Y. M. D. (2015). Strategies for mitigating building collapse in Nigeria: Roles of architects and other stakeholders in the building industry. *Civil and Environmental Research*, *7*(8), 140–148.

Balogun, I. I., Sojobi, A. O., & Galkaye, E. (2017). Public water supply in Lagos State, Nigeria: Review of importance and challenges, status and concerns and pragmatic solutions. *Cogent Engineering*, *4*(1), 1329776. https://doi.org/10.1080/23311916.2017.1329776

Bjerrum, L. (1963). Allowable settlements of structures. *Proceedings of European Conference on Soil Mechanics and Foundation Engineering*, *2*, 135–137.

Blackwell, E., Shirzaei, M., Ojha, C., & Werth, S. (2020). Tracking California's sinking coast from space: Implications for relative sea-level rise. *Science Advances*, *6*(31), 1–10. https://doi.org/10.1126/sciadv.aba4551

Blewitt, G., Hammond, W. C., & Kreemer, C. (2018). Harnessing the GPS data explosion for interdisciplinary science. *Eos*, *99*, 485. https://doi.org/10.1029/2018EO104623

Blewitt, G., Kreemer, C., Hammond, W. C., & Gazeaux, J. (2016). MIDAS robust trend estimator for accurate GPS station velocities without step detection. *Journal of Geophysical Research: Solid Earth*, *121*(3), 2054–2068. https://doi.org/10.1002/2015JB012552

Boateng, F. G. (2020). Building collapse in cities in Ghana: A case for a historical-institutional grounding for building risks in developing countries. *International Journal of Disaster Risk Reduction*, *50*, 101912. https://doi.org/10.1016/j.ijdrr.2020.101912

Boscardin, M., & Cording, E. (1989). Building response to excavation-induced settlement. *Journal of Geotechnical Engineering*, *115*(1), 1–21. https://doi.org/10.1061/(asce)0733-9410(1989)115:1(1)

Burland, J. B., & Wroth, C. P., & Building Research Establishment. (1975). Settlement of buildings and associated damage. Garston, Eng: Building Research Establishment.

Cian, F., Blasco, J. M. D., & Carrera, L. (2019). Sentinel-1 for monitoring land subsidence of coastal cities in Africa using PSInSAR: A methodology based on the integration of SNAP and StaMPS. *Geosciences*, *9*(124), 1–32. https://doi.org/10.3390/geosciences9030124

Cigna, F., & Tapete, D. (2021a). Present-day land subsidence rates, surface faulting hazard and risk in Mexico City with 2014–2020 Sentinel-1 IW InSAR. *Remote Sensing of Environment*, *253*, 112161. https://doi.org/10.1016/j.rse.2020.112161

Cigna, F., & Tapete, D. (2021b). Satellite InSAR survey of structurally-controlled land subsidence due to groundwater exploitation in the Aguascalientes Valley, Mexico. *Remote Sensing of Environment*, *254*, 112254. https://doi.org/10.1016/j.rse.2020.112254

Day, R. (1990). Differential movement of slab-on-grade structures. *Journal of Performance of Constructured Facilities*, *4*(4), 236–241. https://doi.org/10.1061/(asce)0887-3828(1990)4:4(236)

Ebehikhalu, N., & Dawam, P. (2014). Spatial analysis of building collapse in Nigeria: A study of the causes. *Journal of Economics and Sustainable Development*, *5*(25), 95–107.

Ede, A. N. (2010). Building collapse in Nigeria: The trend of casualties in the last decade (2000–2010). *International Journal of Civil & Environmental Engineering* IJCEE-IJENS IJENS, *10*(6), 32–36.

Farr, T. G., Rosen, P. A., Caro, E., Crippen, R., Duren, R., Hensley, S., et al. (2007). The Shuttle radar topography mission. *Reviews of Geophysics*, *45*(2), RG2004. https://doi.org/10.1029/2005RG000183

Fernández-Torres, E., Cabral-Cano, E., Solano-Rojas, D., Emre Havazli, E., & Salazar-Tlaczani, L. (2020). Land Subsidence risk maps and InSAR based angular distortion structural vulnerability assessment: An example in Mexico City. *Proceedings of the International Association of Hydrological Sciences*, *382*, 583–587. https://doi.org/10.5194/piahs-382-583-2020

Fox-Kemper, B., Hewitt, H. T., Xiao, C., Aðalgeirsdóttir, G., Drijfhout, S. S., Edwards, T. L., et al. (2021). Ocean, cryosphere and sea level change. In V. MassonDelmotte, P. Zhai, A. Pirani, S. L. Connors, C. Péan, S. Berger, et al. (Eds.), *Climate change 2021: The physical science basis. Contribution of working group I to the sixth assessment report of the intergovernmental panel on climate change*. Cambridge University Press. In Press.

Hanssen, R. F. (2001). *Radar interferometry, data interpretation and error analysis* (Vol. 328). Kluwer Academic Publishers.

Herrera-García, G., Ezquerro, P., Tomas, R., Béjar-Pizarro, M., López-Vinielles, J., Rossi, M., et al. (2021). Mapping the global threat of land subsidence. *Science*, *371*(6524), 34–36. https://doi.org/10.1126/science.abb8549

Ikuemonisan, F. E., & Ozebo, V. C. (2020). Characterisation and mapping of land subsidence based on geodetic observations in Lagos, Nigeria. *Geodesy and Geodynamics*, *11*(2), 151–162. https://doi.org/10.1016/j.geog.2019.12.006

Kabir, H., Maple, M., Islam, M. S., & Usher, K. (2019). The current health and wellbeing of the survivors of the Rana plaza building collapse in Bangladesh: A qualitative study. *International Journal of Environmental Research and Public Health*, *16*(2342), 1–21. https://doi.org/10.3390/ijerph16132342

Keim, M. (2021). When Buildings Collapse. Disaster doc. Retrieved from https://disasterdoc.org/when-buildings-collapse/

Khorrami, M., Abrishami, S., Maghsoudi, Y., Alizadeh, B., & Perissin, D. (2020). Extreme subsidence in a populated city (Mashhad) detected by PSInSAR considering groundwater withdrawal and geotechnical properties. *Scientific Reports*, *10*(11357), 1–16. https://doi.org/10.1038/s41598-020-67989-1

Lu, X., Guan, H., Sun, H., Li, Y., Zheng, Z., Fei, Y., et al. (2021). A preliminary analysis and discussion of the condominium building collapse in surfside, Florida, US, June 24, 2021. *Frontiers of Structural and Civil Engineering*, *15*(5), 1097–1110. https://doi.org/10.1007/s11709-021-0766-0

Mahmud, M. U., Yakubu, T. A., Adewuyi, T. O., Sousa, J. J., Ruiz-Armenteros, A. M., Bakoň, M., et al. (2016). *Subsidence monitoring in the coastal region of Nigeria using multi-temporal interferometric synthetic aperture radar (MT-InSAR)* (pp. 6–10). European Space Agency, (Special Publication) ESA SP, SP-740.

Miller, M. M., & Shirzaei, M. (2015). Spatiotemporal characterization of land subsidence and uplift in Phoenix using InSAR time series and wavelet transforms. *Journal of Geophysical Research: Solid Earth*, *120*(8), 5822–5842. https://doi.org/10.1002/2015JB012017

Miller, M. M., & Shirzaei, M. (2021). Assessment of future flood hazards for southeastern Texas: Synthesizing subsidence, sea-level rise, and storm surge scenarios. *Geophysical Research Letters*, *48*(8), 1–12. https://doi.org/10.1029/2021GL092544

Minderhoud, P. S. J., Middelkoop, H., Erkens, G., & Stouthamer, E. (2020). Groundwater extraction may drown mega-delta: Projections of extraction-induced subsidence and elevation of the Mekong delta for the 21st century. *Environmental Research Communications*, *2*(1), 011005. https://doi.org/10.1088/2515-7620/ab5e21

Mohamadi, B., Balz, T., & Younes, A. (2020). Towards a PS-InSAR based prediction model for building collapse: Spatiotemporal patterns of vertical surface motion in collapsed building areas—Case study of Alexandria, Egypt. *Remote Sensing*, *12*(20), 1–19. https://doi.org/10.3390/rs12203307

Nicholls, R. J., Lincke, D., Hinkel, J., Brown, S., Vafeidis, A. T., Meyssignac, B., et al. (2021). A global analysis of subsidence, relative sea-level change, and coastal flood exposure. *Nature Climate Change*, *11*(4), 338–342. https://doi.org/10.1038/s41558-021-01064-z

Odeyemi, S. O., Giwa, Z. T., & Abdulwahab, R. (2019). Building collapse in Nigeria (2009–2019), causes and remedies: A review. *USEP: Journal of Science and Engineering Production*, *1*(1), 122–135.

Okagbue, H. I., Iroham, C. O., Peter, N. J., Owolabi, J. D., Patience, I., Adamu, P. I., & Opanuga, A. A. (2018). Systematic review of building failure and collapse in Nigeria. *International Journal of Civil Engineering & Technology*, *10*(10), 1391–1401. Retrieved from http://www.iaeme.com/IJCIET/issues.asp?JTypeIJCIET%26VType=6%26IType=7

Okunola, O. H. (2021). Survival of the fittest: Assessing incidents of building collapse and reduction practices in Lagos, Nigeria. *Environmental Quality Management*, *31*(4), 141–150. https://doi.org/10.1002/tqem.21781

Okunola, O. H. (2022). Quantifying frequent building collapse and disaster risk reduction in Nigeria. Africa in Focus. Retrieved from https://www.brookings.edu/blog/africa-in-focus/2022/04/06/quantifying-frequent-building-collapse-and-disaster-risk-reduction-in-nigeria/

Oloke, O. C., Oni, A. S., Ogunde, A., Opeyemi, J., & Babalola, D. O. (2017). Incessant building collapse in Nigeria: A framework for post-development management control. *Developing Country Studies*, *7*(3), 114–127.

Oloruntola, M., Bayewu, O., Kehinde, K., Obasaju, D. O., & Mosuro, G. O. (2018). Profiles of problematic soils and spatial distribution: Implication on foundation construction in parts of Kosofe Lagos, southwestern Nigeria. *GeoScience Engineering*, *64*(4), 11–22. https://doi.org/10.2478/gse-2018-0017

Oyedele, K. F., Oladele, S., & Okoh, C. (2012). Geo-assessment of subsurface conditions in Magodo brook estate, Lagos, Nigeria. *International Journal of Advanced Scientific and Technical Research*, *4*(2), 731–741. Retrieved from http://www.rspublication.com/ijst/index.html

Ozer, I. E., & Geurts, C. P. W. (2021). Literature review: Effects of subsidence on buildings. (Nederlandse Organisatie voor Toegepast Natuurwetenschappelijk Onderzoek (TNO) final report 2020 No. R12073), (pp. 1–31). Retrieved from https://api.schadedoormijnbouw.nl/content/TNO%202020%20R12073%20Literature%20Review.pdf

Parsons, T. (2021). The weight of cities: Urbanization effects on Earth's subsurface. *AGU Advances*, *2*(1), e2020AV000277. https://doi.org/10.1029/2020AV000277

Restrepo-Ángel, J. D., Mora-Páez, H., Díaz, F., Govorcin, M., Wdowinski, S., Giraldo-Londoño, L., et al. (2021). Coastal subsidence increases vulnerability to sea level rise over twenty first century in Cartagena, Caribbean Colombia. *Scientific Reports*, *11*(1), 1–13. https://doi.org/10.1038/s41598-021-98428-4

Sanya, R., & Mwebaze, E. (2020). Identifying patterns in urban housing density in developing countries using convolutional networks and satellite imagery. *Heliyon*, *12*(6), e05617. https://doi.org/10.1016/j.heliyon.2020.e05617

Shirzaei, M. (2013). A wavelet-based multitemporal DInSAR algorithm for monitoring ground surface motion. *IEEE Geoscience and Remote Sensing Letters*, *10*(3), 456–460. https://doi.org/10.1109/LGRS.2012.2208935

Shirzaei, M., & Bürgmann, R. (2012). Topography correlated atmospheric delay correction in radar interferometry using wavelet transforms. *Geophysical Research Letters*, *39*(1), 1–6. https://doi.org/10.1029/2011GL049971

Shirzaei, M., & Bürgmann, R. (2018). Global climate change and local land subsidence exacerbate inundation risk to the San Francisco Bay Area. *Science Advances*, *4*(3), 1–9. https://doi.org/10.1126/sciadv.aap9234

Shirzaei, M., Freymueller, J., Törnqvist, T. E., Galloway, D. L., Dura, T., & Minderhoud, P. S. J. (2021). Measuring, modelling, and projecting coastal land subsidence. *Nature Reviews Earth & Environment*, *2*(1), 40–58. https://doi.org/10.1038/s43017-020-00115-x

Shirzaei, M., & Walter, T. R. (2011). Estimating the effect of satellite orbital error using wavelet-based robust regression applied to InSAR deformation data. *IEEE Transactions on Geoscience and Remote Sensing*, *49*(11), 4600–4605. https://doi.org/10.1109/TGRS.2011.2143419

Skempton, A. W., & Macdonald, D. H. (1956). The allowable settlements of buildings. *Proceedings of the Institution of Civil Engineers*, *6*(5), 727–768. https://doi.org/10.1680/ipeds.1956.12202

Vassileva, M., Al-Halbouni, D., Motagh, M., Walter, T. R., Dahm, T., & Wetzel, H. U. (2021). A decade-long silent ground subsidence hazard culminating in a metropolitan disaster in Maceió, Brazil. *Scientific Reports*, *11*(1), 1–13. https://doi.org/10.1038/s41598-021-87033-0

Windapo, A. O., & Rotimi, J. O. (2012). Contemporary issues in building collapse and its implications for sustainable development. *Buildings*, *2*(3), 283–299. https://doi.org/10.3390/buildings2030283

Wood, R. H. (1958). The stability of tall buildings. *Proceedings of the Institution of Civil Engineers*, *11*(1), 69–102. https://doi.org/10.1680/iicep.1958.2424

Wu, P., Wei, M., & D'Hondt, S. (2022). Subsidence in coastal cities throughout the world observed by InSAR. *Geophysical Research Letters*, *49*(7). https://doi.org/10.1029/2022GL098477

Zhang, L. M., & Ng, A. M. (2007). *Limiting tolerable settlement and angular distortion for building foundations* (pp. 1–11). Geotechnical special publication. https://doi.org/10.1061/40914(233)18

Zhou, C., Gong, H., Chen, B., Gao, M., Cao, Q., Cao, J., et al. (2020). Land subsidence response to different land use types and water resource utilization in Beijing-Tianjin-Hebei, China. *Remote Sensing*, *12*(3), 457. https://doi.org/10.3390/rs12030457.s

References From the Supporting Information

Chxta [@Chxta] (2021). This is MM2's parking lot. Given the rate of building collapses in Lagos, can someone alert the right people so we don't have another disaster on our hands? [Image attached]. [Tweet]. Twitter. Retrieved from https://twitter.com/chxta/status/1464960946678505481?s=21%26t=tdkGnaIWs3Up9u1xUS1NB